Electrochimica Acta 74 (2012) 235–243

Contents lists available at SciVerse ScienceDirect

Electrochimica Acta

journal homepage: www.elsevier.com/locate/electacta

Laterally enhanced growth of electrodeposited Au to form ultrathin films on nonconductive surfaces

Chiaki Kobayashi [a], Mikiko Saito [b], Takayuki Homma [a,b,*]

[a] Department of Applied Chemistry, Waseda University, Shinjuku, Tokyo 169-8555, Japan
[b] Nanotechnology Research Center, Waseda University, Shinjuku, Tokyo 162-0041, Japan

ARTICLE INFO

Article history:
Received 18 January 2012
Received in revised form 18 April 2012
Accepted 18 April 2012
Available online 26 April 2012

Keywords:
Electrodeposition
Lateral growth
Self-assembled monolayers
Nanogap electrodes

ABSTRACT

We investigated the laterally enhanced growth of electrodeposited Au for fabricating nanogap electrodes. To enhance the lateral growth, we carried out electrodeposition over patterned electrodes onto a SiO_2 surface modified with self-assembled monolayers (SAMs) or dendrimers with amine groups. The morphology and thickness of the Au films were controlled by adjusting deposition conditions such as duration, applied potential, and Au ion concentration in the bath. To investigate the mechanism of the laterally enhanced growth, the surface states of SAM- or dendrimer-modified SiO_2 were analyzed by X-ray photoelectron spectroscopy (XPS). The XPS results indicate the existence of organic molecules and Au ions on the SiO_2 surface, which suggests that laterally enhanced growth is induced by the Au ions coordinated on the amine groups of the organic molecules. To further analyze the mechanism of the laterally enhanced growth, we investigated the relationship between the morphology of the laterally enhanced growth of Au and the amount of Au ions on organic molecules. The laterally enhanced growth of Au is expected to be useful for fabricating thin film nanogap electrodes.

1. Introduction

Deposition of thin metallic films onto nonconductive surfaces by wet processing is an important fabrication technique for various electronic devices and systems. Wet processing techniques such as electrodeposition have attracted much attention since they offer a number of advantages such as high throughput, high accuracy, and high deposition selectivity. In particular, controlling the deposition morphology by optimizing deposition conditions is one of the key technologies for advanced applications in the manufacturing of electronic devices [1–6].

Nanogap electrodes, which have a nanometer-size gap between two electrodes, play an important role in molecular electronics, and fabricating such electrodes with a predetermined gap size is a very important issue in the field. The predetermined molecular-scale gap size permits the use of single molecules, molecular nanowires, and biomolecules such as DNAs or other organic nanomaterials in various devices such as molecular transistors or field-effect transistor sensors. To fabricate nanogap electrodes, photolithography and electrochemical deposition processes have been combined because they offer high yield and the gap size can be controlled on a sub-10-nm scale by adjusting the deposition conditions [7–11]. The nanogaps formed with needle-like surface feature are expected to address individual molecules [9]. However, the resulting electrode surface is not sufficiently smooth to allow fundamental electrical measurement of organic molecules such as organic nanowires or advanced research into the fabrication of organic electronic devices. The rough electrodes tend to physically damage organic materials by aligning them between the gap electrodes. In addition, organic materials cannot easily make an ohmic contact with the electrodes or (because of the electrode thickness) make contact with the insulator surface between the gap electrodes. To improve the reproducibility of measurements of electrical properties and to attain the objective of molecular electronics, it is highly desirable to form thin, smooth electrodes by electrochemical deposition processes.

Although several attempts have been made to achieve anisotropic growth in the vertical direction [12], few studies on anisotropic growth in a lateral direction over an insulator surface from a patterned electrode (we call this as “laterally enhanced growth”) has not been attempted. To form electrodeposits on insulator surfaces, suppression of electrodeposition in the vertical direction have been studied. Argoul et al. attempted thin-layered solution to suppress convection in vertical direction in μm to mm scale [13]. With physically patterning technique, Penner et al. formed thin metallic layer on an insulator surface [14]. Direct plating method also is not laterally enhanced growth because the deposition is induced from an insulator whose resistivity decreased by dispersed metal nanoparticles onto the insulator

* Corresponding author at: Department of Applied Chemistry, Waseda University, 3-4-1 Okubo, Shinjuku, Tokyo 169-8555, Japan.
E-mail address: t.homma@waseda.jp (T. Homma).

0013-4686/$ – see front matter © 2012 Elsevier Ltd. All rights reserved.
http://dx.doi.org/10.1016/j.electacta.2012.04.071

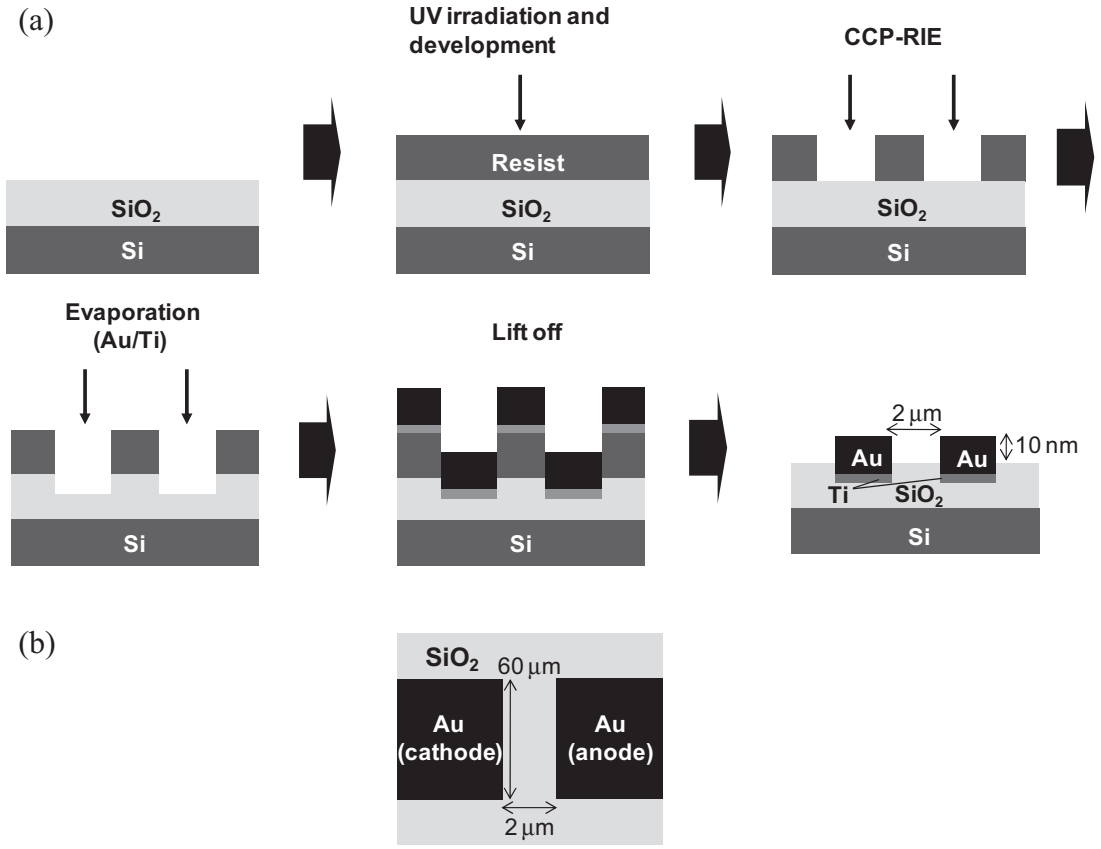

Fig. 1. Fabrication process and structure of microgap electrodes: (a) the cross-sectional model of the fabrication process and (b) the plan view of the electrodes.

surface [15–17]. To control the morphology of the electrodeposited metallic surface, attempts have been made to modify the electrode surface with organic molecular structures such as self-assembled monolayers (SAMs) or dendrimers [18,19]. Such modifications by organic molecular processes allow various surface states to be targeted via the choice of functional groups in the molecular structure.

To fabricate ultrathin metal films, we focused on the surface states of the insulator SiO_2 to enhance the lateral growth of electrodeposited Au [20]. To control the surface states (i.e., surface energy and complexation) with deposited metal ions, amine-terminated SAMs were used to develop a spontaneous surface-modification process. The modified surface is expected to enhance lateral deposition onto the insulator surface. Such control of the morphology and thickness of laterally enhanced anisotropic growth may be applied to fabricating nanogap electrodes. In the present study, we investigated the different morphologies of the laterally enhanced growth of Au by varying electrodeposition conditions and the organic surface-modification process.

2. Experimental

2.1. Fabrication of microgap electrodes

Microgap electrodes were fabricated by conventional photolithographic processes. A Si substrate with a 200-nm-thick thermally grown SiO_2 film was cleaned by the solution consisting of sulfuric acid and hydrogen peroxide (H_2SO_4:H_2O_2 = 4:1) for 10 min. The cleaned SiO_2 surface was coated with resist and developed to form patterns. The patterned SiO_2 was etched ~40 nm deep by capacitively coupled plasma reactive-ion etching (CCP-RIE), followed by coating with 10-nm-thick Ti and 50-nm-thick Au, as shown in Fig. 1a. Finally, the resist with the metals was lifted off to form electrodes with 2 μm gap. As shown in Fig. 1b, one electrode was used as a cathode and the other as an anode in the electrodeposition process.

2.2. Formation of organic monolayers

Prior to electrodeposition and X-ray photoelectron spectroscopy (XPS) measurements, SAMs or dendrimers were formed or deposited on the SiO_2 surface by the following process; after the microgap electrodes were cleaned with O_2 plasma for 5 min, the substrate was immersed in solutions containing the SAM constituent or dendrimers for 10 min at 60 °C or 24 h at room temperature, respectively. The SAM solution contained 1.0 vol% of 3-aminopropyltrimethoxysilane (APTES; Kanto Kagaku, Japan) in toluene. The dendrimer solution contained 100 μvol% of generation-8 polyamidoamine (PAMAM; Kanto Kagaku, Japan) in ethanol. The organic molecular structures are shown in Fig. 2. After forming SAMs or depositing dendrimers onto the SiO_2 surface, the substrate was rinsed in an ultrasonic ethanol bath for 10 min and dried under N_2 flow.

2.3. Electrodeposition process

In this study, Au baths containing either cyanide Au or chlorauric acid were used to examine the enhanced lateral deposition. The main difference between these two bath systems is the complexing condition, that is, the deposition potential of Au. Cyanide Au ions are much more stable than Au ions in chlorauric acid. The

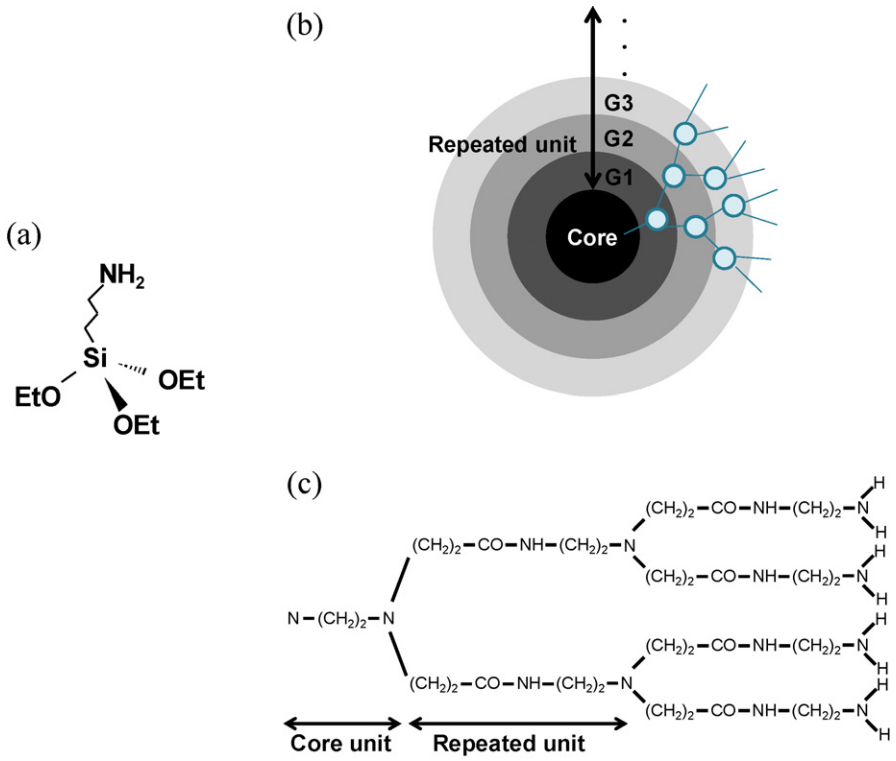

Fig. 2. The molecular structures of APTES and PAMAM: (a) the molecular structure of APTES, (b) the schematic structure of PAMAM and (c) the partial structure of core unit and repeated unit of PAMAM.

cyanide bath consisted of 6.7 g/dm^3 of $KAu(CN)_2$ and 1.1 g/dm^3 of $K_2[Ni(CN)_4]$ to reduce the grain size of the deposited Au. The pH was adjusted to neutral using H_3PO_4 to prevent hydrolysis of the SAMs, which occurs under high pH conditions. The chlorauric-acid baths contained concentrations of 0.16 g/dm^3, 0.8 g/dm^3, or 4.0 g/dm^3 of $HAuCl_4{\cdot}4H_2O$. All electrodeposition experiments were performed in a three-compartment electrochemical cell using a digital potentiostat (Hokuto Denko, HZ-5000). The electrode potential is relative to a Ag/AgCl (saturated with KCl) electrode. To investigate Au deposition, one electrode was used as a counter electrode and the other as a working electrode. After modifying the SiO_2 surface, as described in Section 2.2, electrodeposition was performed at room temperature for deposition durations between 3 s and 30 s. The surface morphology of the deposits was observed by scanning electron microscope (SEM).

2.4. X-ray photoelectron spectroscopy process

After the SiO_2 surface modified with organic molecules was immersed into cyanide-Au or chlorauric-acid baths, XPS measurements were performed. The samples were immersed in a cyanide-Au bath for 30 s and in chlorauric-acid baths for 0 s, 5 s, 10 s, and 30 s, respectively. To analyze the mechanism of laterally enhanced growth, Au electrodeposition was performed on samples covered with different coverage of SAM species. The microgap electrodes modified with APTES-SAMs were immersed into KOH solution for 0 s, 45 s, 90 s, and 300 s to partially remove the SAMs.

XPS spectra were obtained using an ULVAC-PHI 5400 ESCA System X-ray photoelectron spectrometer with Al Kα radiation. The base pressure in the analysis chamber was 5×10^{-10} Torr. Narrow-scan spectra of the N-1*s* and Au-4*f* spectral regions were obtained with a pass energy of 35.75 eV, an electron-beam power of 400 W, and a resolution of 0.2 eV. The binding energy was calibrated with O_2-1*s* peak at 84.0 eV.

3. Results and discussion

The laterally enhanced growth of Au was observed using both the cyanide-Au bath and the chlorauric-acid bath, and the differences in morphology and thickness of the resulting deposits were investigated. In particular, we systematically changed parameters of electrodeposition using chlorauric-acid bath and analyze the influences of the deposition conditions to the lateral growth on the APTES-modified SiO_2.

3.1. Electrodeposition using cyanide bath

Linear-sweep voltammetry (LSV) was carried out with the samples immersed in the cyanide-Au bath or chlorauric-acid bath (see Fig. 3). From the LSV, we estimate the deposition potential of Au from cyanide-Au to be approximately −600 mV, and we find

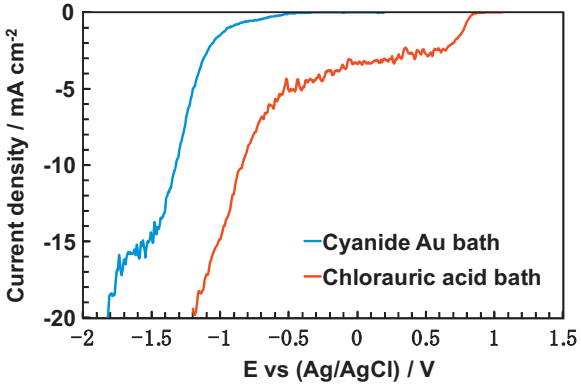

Fig. 3. Linear sweep voltammograms for the cyanide Au-electrodeposition bath and chlorauric-acid Au-electrodeposition bath.

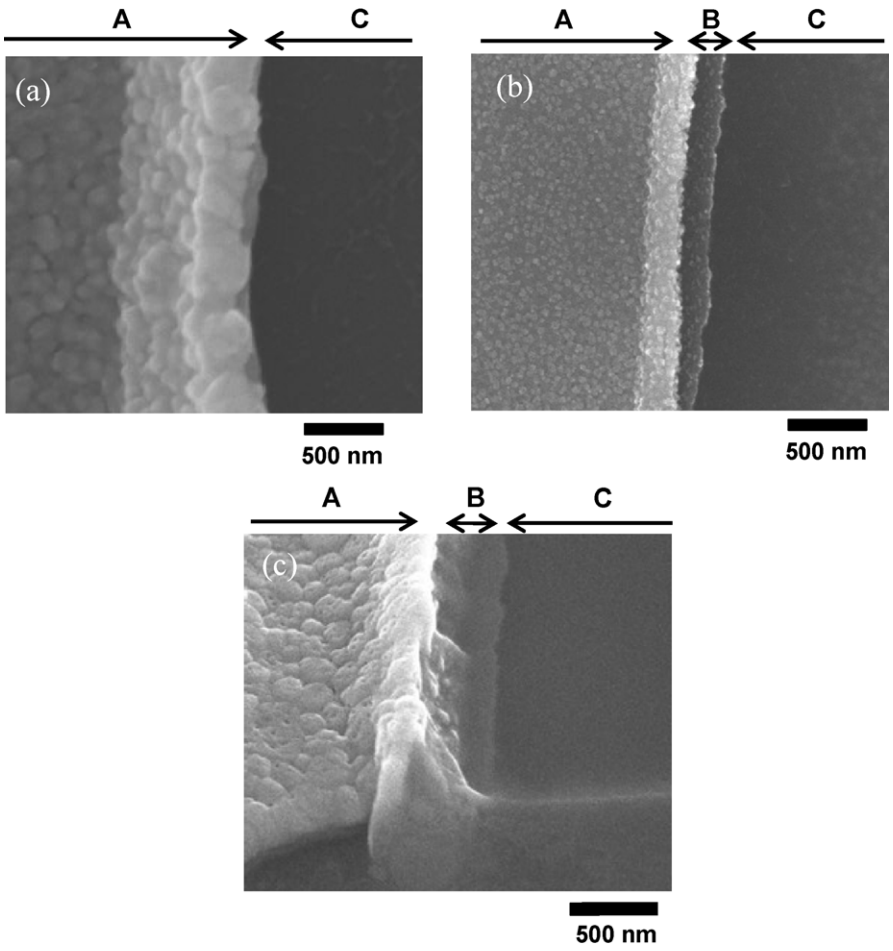

Fig. 4. Scanning electron micrographs of Au electrodeposited at −1200 mV for 10 s. Panel (a) shows Au deposited on a non-modified SiO_2 surface (plan view), panels (b) and (c) show a plan view and an 60° inclined view, respectively, of Au deposited on a PAMAM-modified SiO_2 surface. Labels A, B, and C indicate the original electrode, the laterally enhanced growth area, and the SiO_2 surface, respectively.

a large increase in the current due to hydrogen evolution above the −1700 mV region. Thus, we performed electrodeposition with applied voltage up to −1700 mV.

First, after modifying the SiO_2 surface with PAMAM, Au electrodeposition was performed at −1200 mV for 10 s, and differences between the non-modified SiO_2 surface and the PAMAM-modified SiO_2 surface were observed (see Fig. 4). On the non-modified surface (Fig. 4a), bright-contrast parts are observed and interpreted as preferential Au growth at the edge of the electrode due to the so-called "edge effect." In contrast, we observe laterally enhanced growth beyond this region (Fig. 4b). Judging from the inclined view (Fig. 4c), the electrodeposited layer is very thin and smooth which suggests enhanced growth in the lateral direction. The deposition should occur not only on PAMAM molecules but also in PAMAM molecules [21].

Next, we performed XPS measurements to study the condition of the dendrimer layers and the Au ions coordinated to the organic molecules. XPS spectra from PAMAM-modified SiO_2 surfaces were acquired after immersing the substrate in a cyanide-Au electrodeposition bath for 30 s (Fig. 5). In Fig. 5a, N-1*s* peaks, which are attributed to the amine group of the organic molecules, are observed. Moreover, as shown Fig. 5b, Au-4*f* peaks are observed, whereas these peaks are not observed for the non-modified substrates. We attribute the Au-4*f* peaks to Au ions adsorbed onto the amine groups. Because the adsorbed Au ions were expected to enhance the lateral growth onto the insulator surface, we investigated in detail the relationship between the concentration of Au ions and the laterally enhanced growth of Au using the chlorauric-acid bath.

3.2. Electrodeposition using chlorauric-acid bath

To lengthen the laterally enhanced growth, we attempted to apply chlorauric acid to the electrodeposition bath. Chlorauric Au ions adsorb more easily onto amine groups than when using cyanide ions because of their different complex stability. The result of LSV indicated that Au starts to deposit at approximately +800 mV when using the chlorauric-acid bath (Fig. 3), which indicates that, as expected, Au ions are less stable in the chlorauric-acid bath than in the cyanide-Au bath. We investigated morphological change of the laterally enhanced growth on PAMAM- or APTES-modified SiO_2 with varying electrodeposition condition.

After modifying the SiO_2 surface with PAMAM, electrodeposition was performed at +550 mV for 10 s. We observe laterally enhanced growth from the edge of the electrode, as shown in Fig. 6. In this figure, the parts labeled A, B, and C indicate the original Au electrode, the laterally enhanced Au growth, and SiO_2 surface, respectively. Judging from the top view (Fig. 6a), the laterally enhanced growth is rougher, compared with the results obtained with the cyanide bath (described above), and lateral growth onto the SiO_2 surface is longer than that for the cyanide bath. Laterally enhanced growth is clearly observed in the angled SEM image of the identical sample, as shown in Fig. 6b. However, for

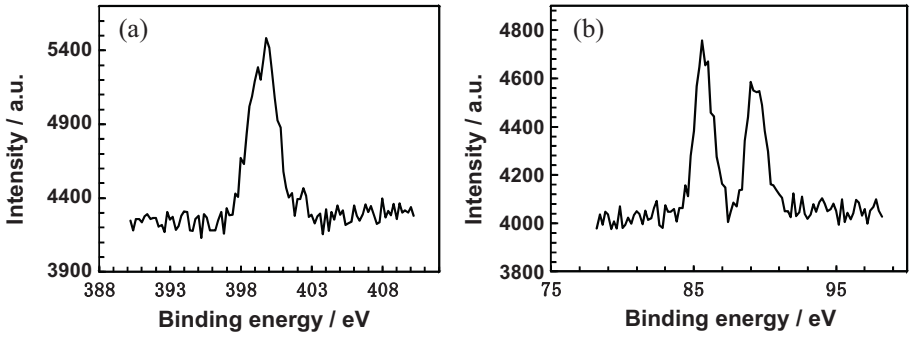

Fig. 5. X-ray photoelectron spectra of (a) N-1*s* and (b) Au-4*f* regions from PAMAM-modified SiO_2 after 30-s immersion into cyanide-Au electrodeposition bath.

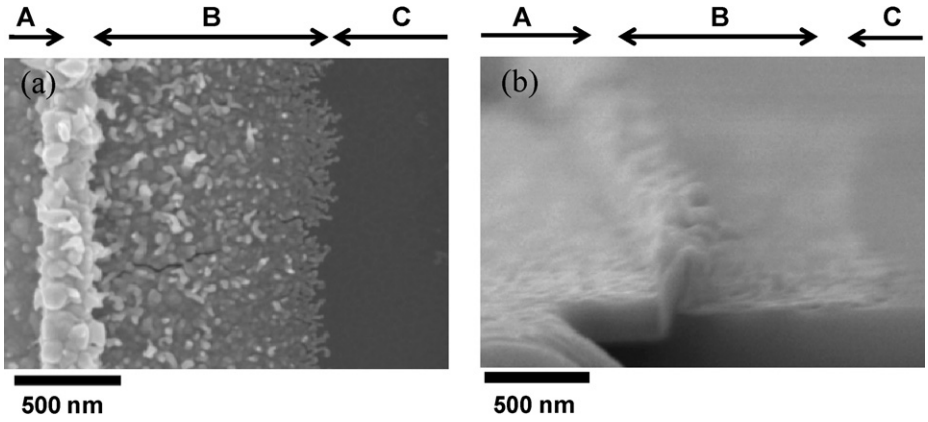

Fig. 6. Scanning electron micrographs of Au electrodeposited on PAMAM-modified SiO_2 at +550 mV for 10 s. Panel (a) shows a plan view and panel (b) shows an 85° inclined view. Labels A, B, and C indicate the original electrode, the laterally enhanced growth area, and the SiO_2 surface, respectively.

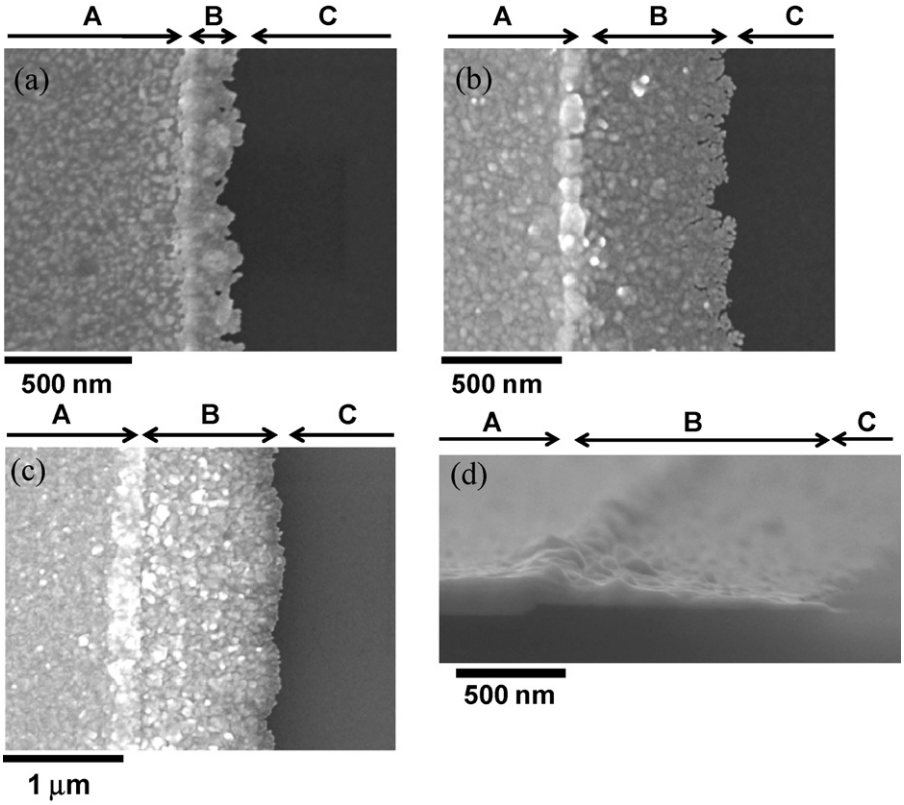

Fig. 7. Scanning electron micrographs of Au electrodeposited onto APTES-SAM-modified SiO_2 at +500 mV. Deposition durations are (a) 5 s, (b) 20 s, and (c and d) 30 s. Panels (a)–(c) are plan views and (d) is an 85° inclined view. Labels A, B, and C indicate the original electrode, the laterally enhanced growth area, and the SiO_2 surface, respectively.

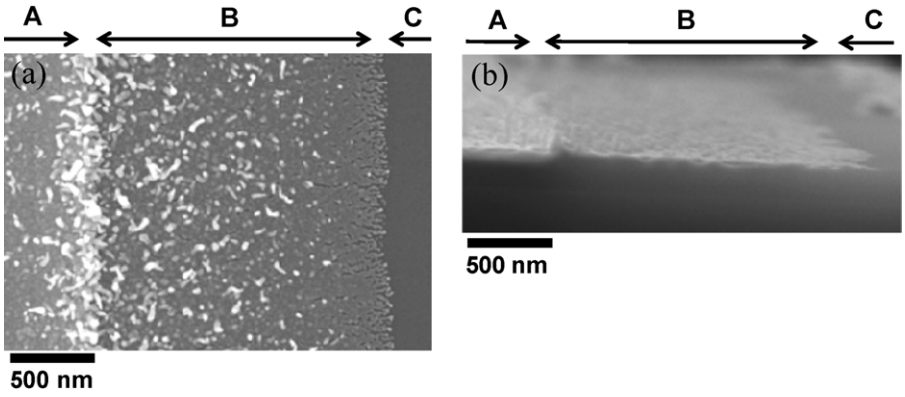

Fig. 8. Scanning electron micrograph of Au electrodeposited onto an APTES-SAM-modified SiO_2 surface at +200 mV for 5 s. Panel (a) is a plan view and panel (b) is an 85° inclined view. Labels A, B, and C indicate the original electrode, the laterally enhanced growth area, and the SiO_2 surface, respectively.

applications involving nanogap electrodes, the "isotropically grown part" at the edge of the Au electrode should be suppressed. Thus, thinner electrodes (ca. 10 nm) were used for the following experiments of electrodeposition.

To investigate the influence on the laterally enhanced growth of the applied potential, the Au ion concentration, and the organic molecule surface coverage, APTES-SAM-modified SiO_2 samples were prepared using Au electrodeposition from a chlorauric-acid bath. The main differences between the APTES- and PAMAM-modification processes are the total amount of Au ions that bind to the amine groups and the coverage of the SiO_2 surface by the organic molecules. Although the total amount of Au ions bound to PAMAM is larger than that bound to APTES, the coverage of PAMAM on SiO_2 is expected to be less than that of APTES because the Coulomb binding is weaker than the covalent binding [22]. For this reason, we compared the morphology of the deposits with laterally enhanced growth onto PAMAM- and APTES-SAM-modified SiO_2 to analyze how Au ions are distributed over the modified SiO_2 surfaces.

APTES-SAM-modified SiO_2 was applied to the electrodeposition at +500 mV for 5 s, 20 s, and 30 s, and the laterally enhanced growth of the film structure was observed on each substrate (see Fig. 7). The laterally enhanced growth of the Au film on the APTES-SAM-modified SiO_2 surface is smoother than that of the Au film on the PAMAM-modified SiO_2 surface (c.f. Fig. 6). The cross-sectional view shown in Fig. 7d indicates that the thickness of the tip of the laterally enhanced growth part is thinner (approximately 30 nm), than that of the part near the original electrode. These results indicate that isotropic growth occurs concurrently with lateral growth.

To investigate the influence of the applied potential on the APTES-SAM-modified surface, electrodeposition was performed at +200 mV for 5 s. Fig. 8 shows clear, laterally enhanced growth results. The inclined view (Fig. 8b) shows that the deposited structure is not sloped like the structure electrodeposited at +500 mV (c.f. Fig. 7d). These results suggest that laterally enhanced growth dominates for more negative (or less positive) potentials, for which isotropic growth is suppressed. In addition, Au ions coordinated with amine groups are expected to be more easily reduced with a more negative potential, which would explain the enhanced lateral growth (see Fig. 9).

To investigate the laterally enhanced growth mechanism for Au, XPS spectra were obtained from an APTES-SAM-modified SiO_2 surface before and after immersion into a chlorauric-acid electrodeposition bath for various immersion durations (Fig. 10). With an increase in the bath-immersion times, the intensity of the N-1*s* peaks slightly decreases; however, the organic molecules are deposited on the SiO_2 surface even for 30-s immersion times. In contrast, the intensity of the Au-4*f* peaks slightly increases with an increase in the bath-immersion time. These results suggest that the organic molecules on the modified SiO_2 surface are desorbed in the chlorauric-acid bath, but the other free Au ions in the bath continue to be adsorbed onto the free amine groups. For this reason, electrodeposition onto the SAM-modified SiO_2 surface from the chlorauric-acid bath was conducted for less than 30 s so as not to perturb the enhanced lateral growth of Au onto the modified SiO_2 surface.

Next, we investigated the influence of the concentration of Au ion in the bath on the lateral growth of Au electrodeposition. For this, Au was electrodeposited onto APTES-SAM-modified SiO_2 using the bath containing 0.16 g/dm^3, 0.8 g/dm^3, and 4.0 g/dm^3 of chlorauric acid. For each concentration, laterally enhanced growth was observed (Fig. 11). With lower concentrations of Au ions, the laterally enhanced growth takes on a dendritic structure, which suggests that deposition occurs under extremely limited diffusion conditions (Fig. 11a and b). In contrast, with higher concentration of Au ions, the laterally enhanced growth forms a densely packed film (Fig. 11c–f).

Fig. 12 shows Au-4*f* XPS spectra of various samples, which were APTES-SAM-modified SiO_2 surfaces immersed into an electrodeposition bath. The spectra indicate that approximately the same amount of Au is adsorbed, regardless of the chlorauric acid concentration in the bath. This XPS result and those shown in Fig. 11 indicate that the morphology and length of the laterally enhanced growth are influenced not only by the Au ions adsorbed onto the SiO_2 surface but also by the Au ions in the electrodeposition bath.

To further investigate the role of SAMs or dendrimers in enhancing the laterally enhanced growth, we investigated the surface

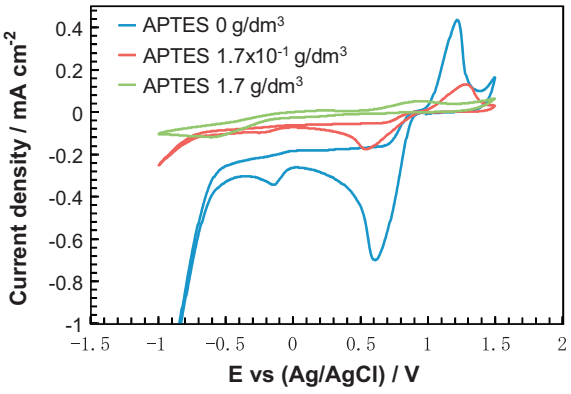

Fig. 9. Cyclic voltammograms for the chlorauric-acid bath containing APTES molecules in various concentrations without stirring bath.

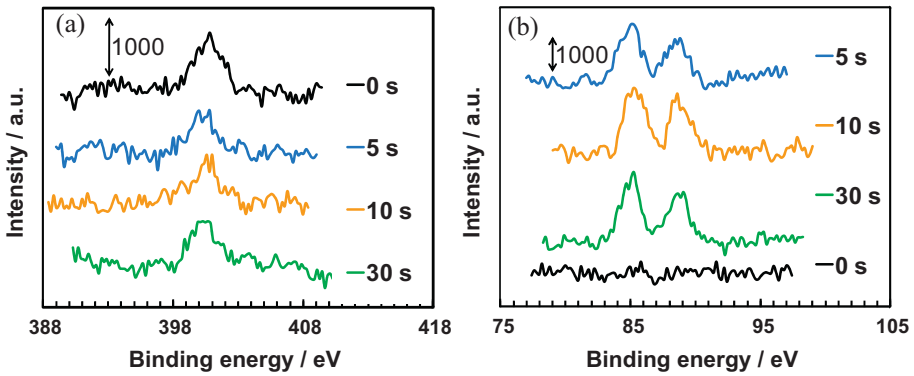

Fig. 10. X-ray photoelectron spectra of the (a) N-1*s* and (b) Au-4*f* spectral regions for APTES-SAM-modified SiO_2 after immersion in a chlorauric-acid electrodeposition bath for 0 s, 5 s, 10 s, and 30 s.

morphology of the deposited Au. To vary the SAM coverage, we exploited the hydrolysis reaction between APTES and SiO_2 (i.e., Si–O–Si and OH^- under high pH), by immersing the APTES-SAM-modified electrodes into a KOH solution for durations of 45 s, 90 s, and 300 s. After immersion into the KOH solution, the substrate was rinsed with pure water and immersed in the chlorauric-acid electrodeposition bath to determine the amount of Au ions on the SAMs.

The change in the SAM coverage and the amount of Au ions bound to the SAMs were evaluated by XPS (Fig. 13). The

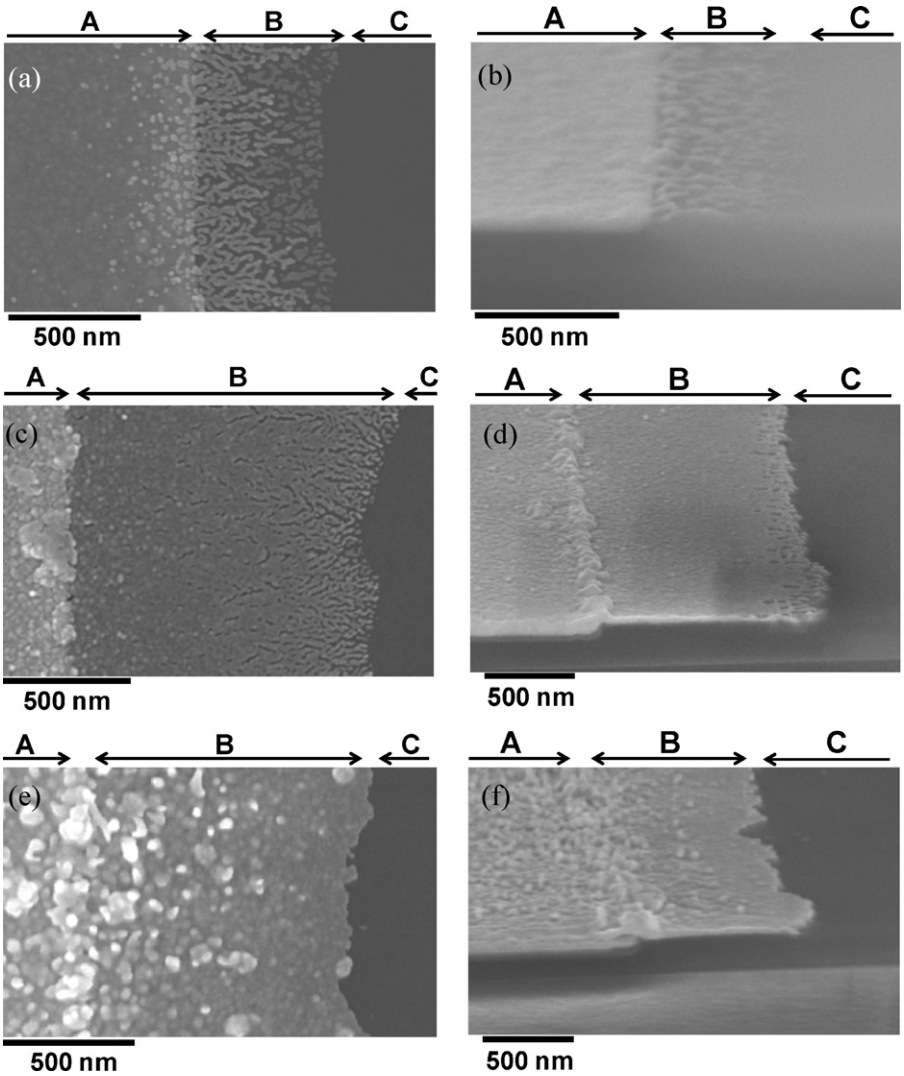

Fig. 11. Scanning electron micrographs of Au electrodeposited onto APTES-SAM-modified SiO_2 at +200 mV for 3 s using different concentrations of $HAuCl_4{\cdot}4H_2O$. Concentrations of $HAuCl_4{\cdot}4H_2O$ are (a and b) 0.16 g/dm^3, (c and d) 0.8 g/dm^3, and (e and f) 4.0 g/dm^3. Panels (a), (c), and (e) are plan views and panels (b), (d), and (f) are 75° inclined views. Labels A, B, and C indicate the original electrode, the laterally enhanced growth area, and the SiO_2 surface, respectively.

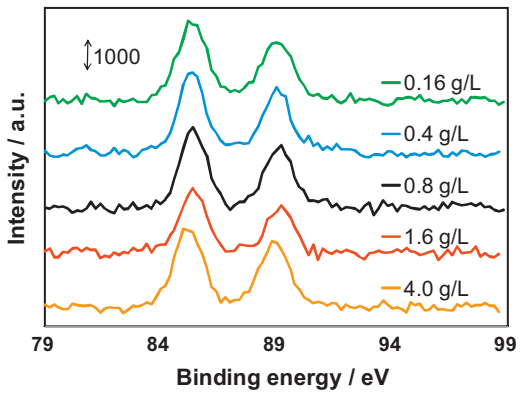

Fig. 12. X-ray photoelectron spectra of Au-4*f* spectral region for X-ray photoelectron spectra of Au-4*f* spectral region for immersion into an electrodeposition bath using different concentrations of $HAuCl_4{\cdot}4H_2O$ for 30 s. From upper to lower curves, concentrations are 0.16 g/dm^3, 0.4 g/dm^3, 0.8 g/dm^3, 1.6 g/dm^3 and 4.0 g/dm^3, respectively.

intensities of the N-1*s* and Au-4*f* peaks decreased with an increase in the immersing duration of the substrate in KOH solution. The relative concentration of Au ions adsorbed on the SAMs after the immersion was estimated by integrating the Au peaks, normalized to the XPS-peak area from Au ions adsorbed when the sample was not immersed in KOH solution. From this result, relative coverage of SAM with the KOH immersions of 45 s, 90 s, and 300 s can be estimated as 0.70, 0.39, and 0.0, respectively.

After partial removal of the SAMs, electrodeposition was performed at +200 mV. The SEM images of the samples (Fig. 14) show that the laterally enhanced growth is suppressed with an increase in the immersion time in the KOH solution, i.e., the decrease in coverage of the SAM. We estimated the relative length of the laterally enhanced growth for various KOH-immersion times, again normalizing the length of the laterally enhanced growth to the length without immersion. The relative lengths of the laterally enhanced growth for KOH-immersion times of 45 s, 90 s, and 300 s are 0.67, 0.33, and 0.0, respectively, which agree well with the relative concentration of Au ions adsorbed onto the SiO_2 surface by binding with the amine groups of the SAMs. However, the relative strength

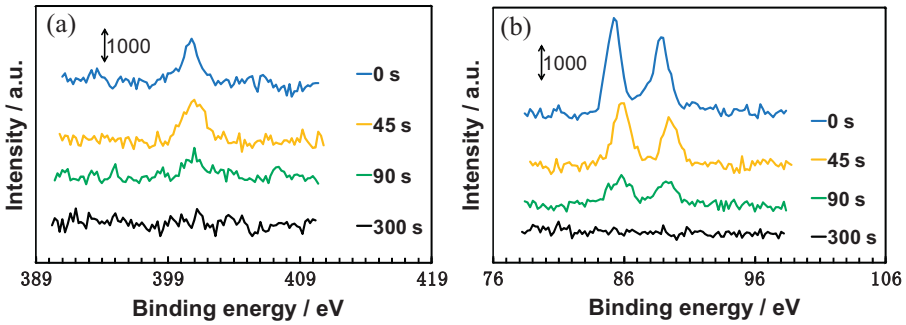

Fig. 13. X-ray photoelectron spectra of (a) N-1*s* and (b) Au-4*f* regions for APTES-SAM-modified SiO_2 after immersion into KOH solution (pH > 13.5) for 0 s, 45 s, 90 s, and 300 s and after 30-s immersion into a chlorauric-acid Au-electrodeposition bath.

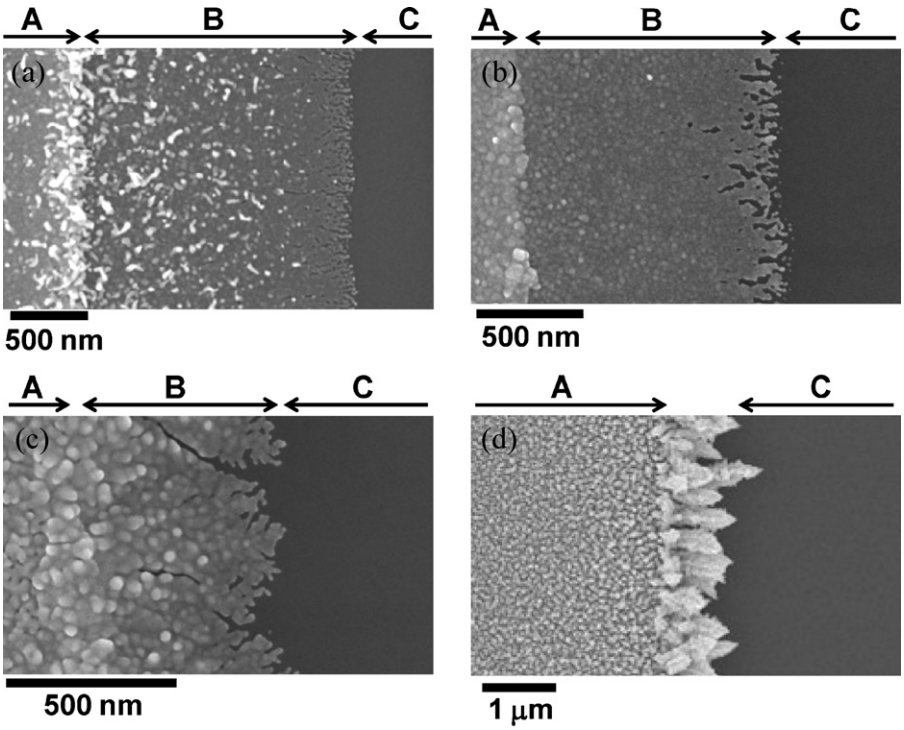

Fig. 14. Scanning electron micrographs of Au electrodeposited at +200 mV after immersion into KOH solution for (a) 0 s, (b) 45 s, (c) 90 s, and (d) 300 s. Deposition durations are (a)–(c) 5 s and (d) 20 s. Labels A, B, and C indicate the original electrode, the laterally enhanced growth area, and the SiO_2 surface, respectively.

of the N-1*s* peak, which originates from the amine groups, does not correspond to the relative length of the laterally enhanced growth. These results indicate that the lateral growth is enhanced mainly by the Au ions absorbed onto the APTES-SAMs on the SiO_2 and not the amine groups of the APTES-SAMs.

4. Conclusions

We investigated laterally enhanced growth by electrodeposition of Au onto a SiO_2 surface modified with amine-terminated organic molecules. We observed laterally enhanced growth using both the cyanide Au ions and the chlorauric-acid baths and find that the growth is more easily enhanced using chlorauric-acid baths due to the less stable electrochemical state. The morphology of the laterally enhanced growth depends on the organic molecules that modify the SiO_2 surface, the applied potential, and the concentration of Au ions in the electrodeposition bath. By studying different coverage factors of APTES-SAM-modified SiO_2, we find that the length of the laterally enhanced growth depends on the concentration of the Au ions adsorbed to the SAM-covered surfaces.

Modifying the SiO_2 surface states allows the formation of a thin and smooth Au film whose thickness and morphology can be adjusted by tuning the electrodeposition conditions. Such laterally enhanced growth is expected to be useful for fabricating nanogap electrodes with thin, smooth electrodes.

Acknowledgements

This work was carried out at the "Center for Practical Chemical Wisdom" in the Global-COE Program, MEXT, Japan, and was financially supported in part by Grant-in-Aid for Scientific Research, MEXT, Japan.

References

[1] T.P. Moffat, J.E. Bonevich, W.H. Huber, A. Stanishevsky, D.R. Kelly, G.R. Stafford, D. Josell, Journal of the Electrochemical Society 147 (2000) 4524.
[2] Y. Wang, Y. Cao, M. Wang, S. Zhong, M.Z. Zhang, Y. Feng, R.W. Peng, X.P. Hao, N.B. Ming, Physical Review E 69 (2004) 021607.
[3] R. Qiu, X.L. Zhang, R. Qiao, Y. Li, Y.I. Kim, Y.S. Kang, Chemistry of Materials 19 (2007) 4174.
[4] S.-K. Kim, S.K. Cho, J.J. Kim, Y.-S. Lee, Electrochemical and Solid-State Letters 8 (2005) C19.
[5] J.W. Hsu, W.M. Clift, L.N. Brewer, Langmuir 24 (2008) 5375.
[6] L. Guo, P.C. Searson, Langmuir 24 (2008) 10557.
[7] B. Liu, J. Xiang, J.-H. Tian, C. Zhong, B.-W. Mao, F.-Z. Yang, Z.-B. Chen, S.-T. Wu, Z.-Q. Tian, Electrochimica Acta 50 (2005) 3041.
[8] F. Chen, Q. Qing, L. Ren, Z. Wu, Z. Liu, Applied Physics Letters 86 (2005) 123105.
[9] Z. Yi, M. Banzet, A. Offenhäusser, D. Mayer, Physica Status Solidi (RRL) 4 (2010) 73.
[10] Q. Qing, F. Chen, P. Li, W. Tang, Z. Wu, Z. Liu, Angewandte Chemie-International Edition 44 (2005) 7771.
[11] J.-H. Tian, Y. Yang, B. Liu, B. Sch, D.-Y. Wu, E. Maisonhaute, A.S. Muns, Y. Chen, C. Amatore, N.-J. Tao, Z.-Q. Tian, Nanotechnology 21 (2010) 274012.
[12] Y. Nakamaru, H. Honma, Transactions of the Institution of Metal Finishing 87 (2009) 259.
[13] J.M. Huth, H.L. Swinney, W.D. McCormick, A. Kuhn, F. Argoul, Physical Review E 51 (1995) 3444.
[14] E.J. Menke, M.A. Thompson, C. Xiang, L.C. Yang, R.M. Penner, Nature Materials 5 (2006) 914.
[15] D. Weng, U. Landau, Journal of the Electrochemical Society 142 (1995) 2598.
[16] J.J. Kim, S.-K. Kim, Y.S. Kim, Journal of the Electrochemical Society 151 (2004) C97.
[17] W. Gui-xiang, L. Ning, H. Hui-li, Y. Yuan-chun, Applied Surface Science 253 (2006) 480.
[18] E.D. Eliadis, R.C. Nuzzo, A.A. Gewirth, R.C. Alkire, Journal of the Electrochemical Society 144 (1997) 96.
[19] D. Arrington, M. Curry, S. Street, G. Pattanaik, G. Zangari, Electrochimica Acta 53 (2008) 2644.
[20] C. Kobayashi, S. Yoshida, M. Saito, Y. Wakayama, T. Homma, The Electrochemical Society Transactions 25 (2010) 29.
[21] M.R. Knecht, M.G. Weir, A.I. Frenkel, R.M. Crooks, Chemistry of Materials 20 (2008) 1019.
[22] B.P. Cahill, G. Papastavrou, G.J. Koper, M. Borkovec, Langmuir 24 (2008) 465.